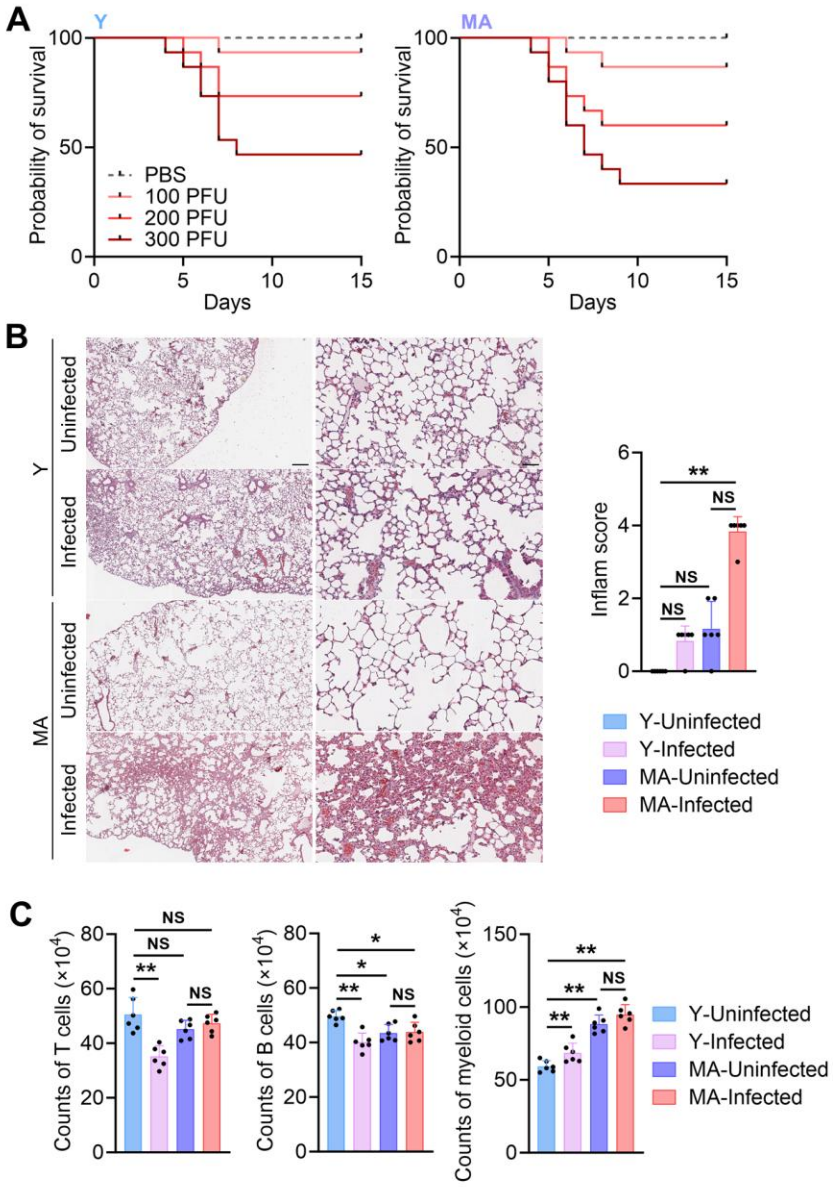
SUPPLEMENTARY DATA

Targeting Mitochondrial MAVS Signaling in Deep-Senescent Hematopoietic Stem Cells Ameliorates Infection-Driven Immunosenescence

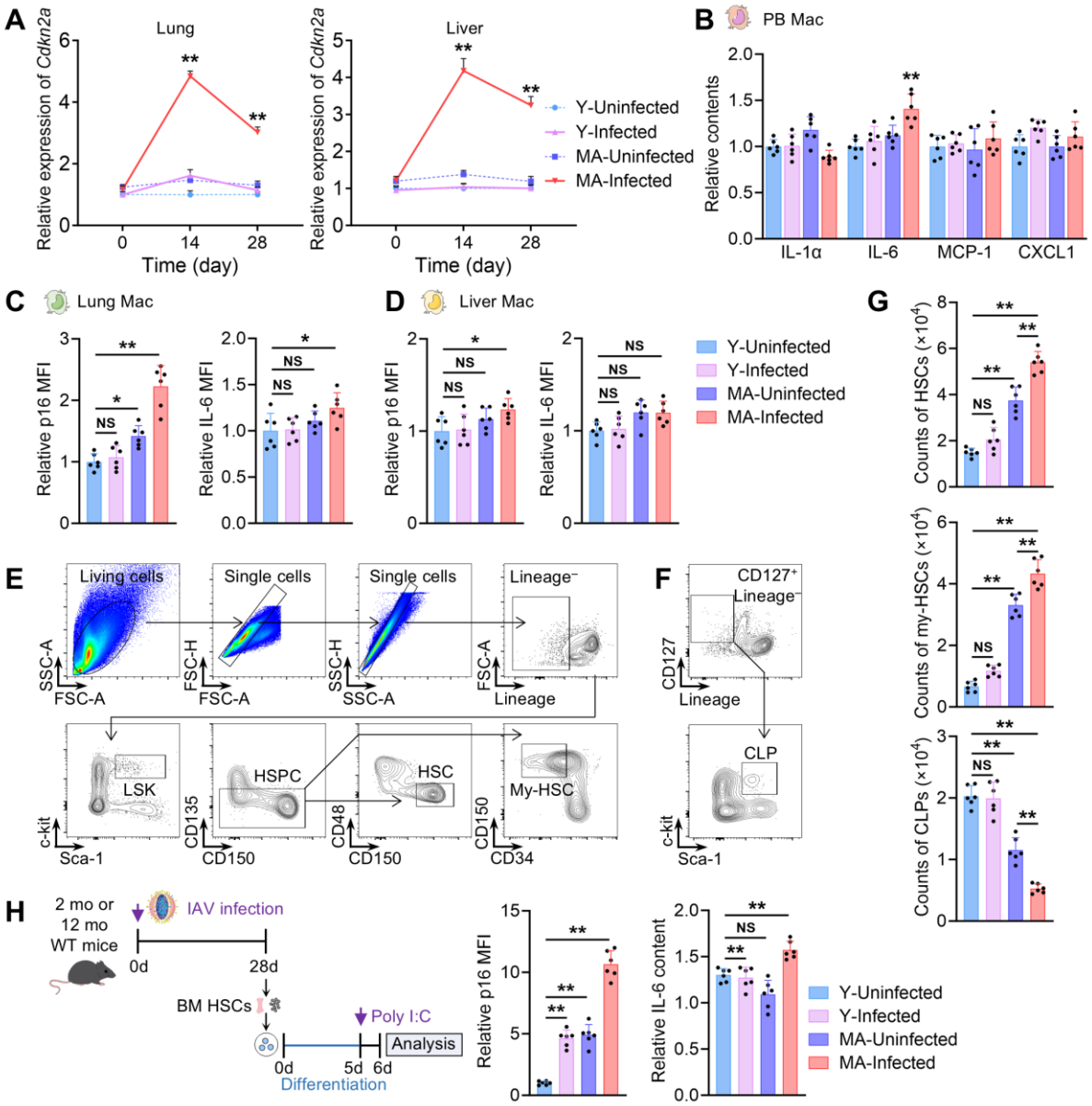
Weinian Liao, Yue Zhang, Yetong Wang, Ruzhou Zhao, Cheng Xu, Tianyue Wang, Mingyang Xie, Zhang Zhang, Xiaodong Zai, Zhongyi Wang, Jun Zhang, Junjie Xu

© 2026. Liao W. et al. Published online at http://www.aginganddisease.org/EN/10.14336/AD.2026.0944



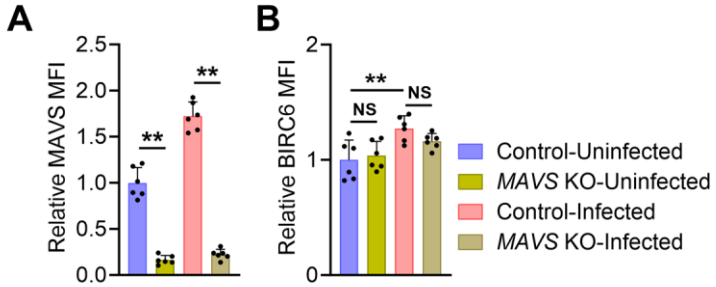
Supplementary Figure 1. IAV infection induces dose-dependent survival outcomes and dynamic pulmonary inflammation in mice. (A) Survival curves of Y and MA mice infected with different IAV doses (n = 15). (B) Lung histology and inflammation scores at 7 dpi (n = 6). Scale bars, 100 μm. (C) The number of T cells, B cells, and myeloid cells in the lung at 28 dpi (n = 6). All quantitative data are presented as mean ± SD, one-way ANOVA with Tukey-Kramer post hoc testing was used for multi-group comparisons unless stated otherwise. Non-parametric alternatives are used for statistical tests, and Kruskal-Wallis test with Dunn's post hoc correction for multi-group comparison in (B). *P < 0.05, **P < 0.01. IAV, influenza A virus; Y, young; MA, middle-aged; dpi, days post-infection.

© 2026. Liao W. et al. Published online at http://www.aginganddisease.org/EN/10.14336/AD.2026.0944

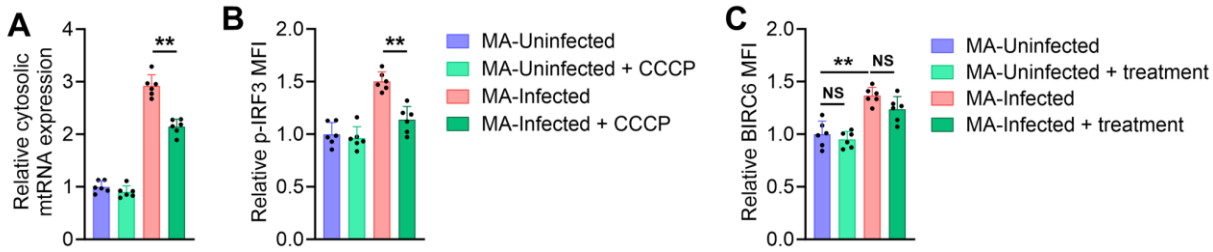


Supplementary Figure 2. IAV infection triggers systemic senescence and functional propagation of HSC senescence. (A) qRT-PCR quantification of *Cdkn2a* expression in liver and lung tissues from Y and MA mice at 28 dpi ($n = 6$). (B) SASP factor levels (IL-1α, IL-6, MCP-1, CXCL1) of sorted peripheral macrophages from Y and MA mice at 28 dpi ($n = 6$). (C, D) Flow cytometric quantification of p16 and IL-6 expression in (C) lung macrophages or (D) liver macrophages from Y and MA mice at 28 dpi ($n = 6$). (E, F) Gating strategy used to assess HSCs, my-HSCs, CLPs in the BM of Y and MA mice. (G) The number of HSCs, my-HSCs, CLPs in the BM at 28 dpi ($n = 6$). (H) Experimental schema and flow cytometric analysis of HSC-derived macrophage. BM HSCs isolated at 28 dpi were differentiated into macrophages and stimulated with Poly(I:C), followed by p16 and IL-6 quantification ($n = 6$). All quantitative data are presented as mean ± SD, one-way ANOVA with Tukey-Kramer post hoc testing was used for multi-group comparisons, $^{*}P < 0.05$, $^{**}P < 0.01$.

© 2026. Liao W. et al. Published online at http://www.aginganddisease.org/EN/10.14336/AD.2026.0944

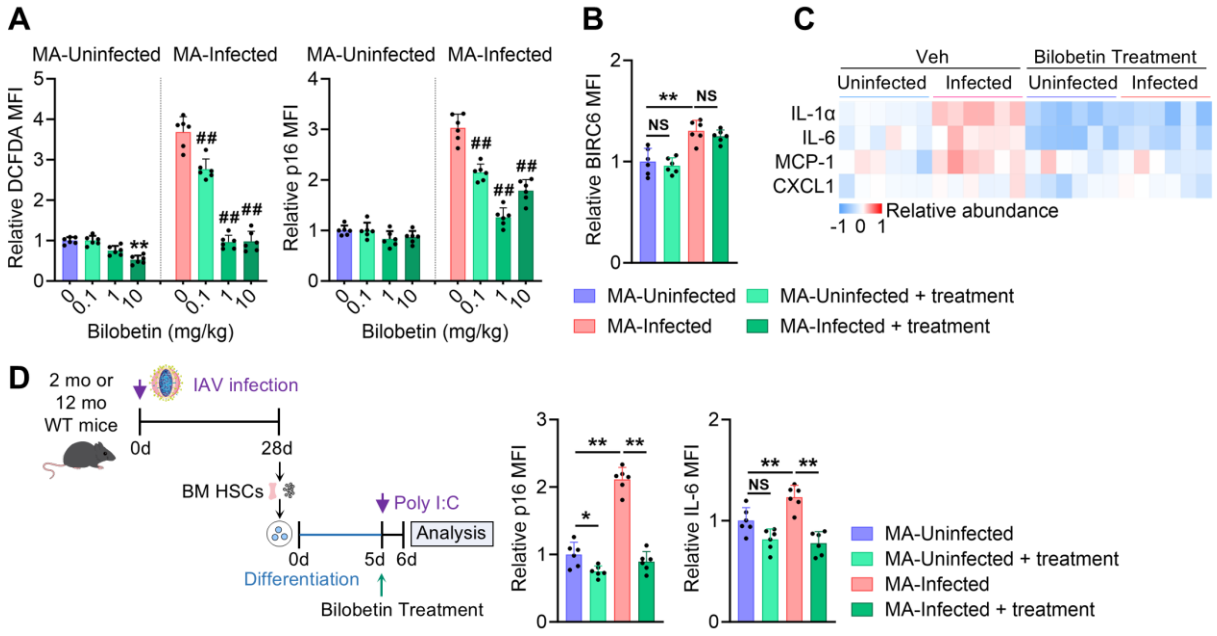


Supplementary Figure 3. Efficient MAVS ablation is achieved in HSCs of conditional knockout mice. (A) Flow cytometric quantification of MAVS expression in HSCs from the BM of control and MAVS conditional knockout mice at 28 dpi (n = 6). (B) Flow cytometric quantification of BIRC6 expression in HSCs from the BM of control and MAVS conditional knockout mice at 28 dpi (n = 6). All quantitative data are presented as mean ± SD, one-way ANOVA with Tukey-Kramer post hoc testing was used for multi-group comparisons, *P < 0.05, **P < 0.01.



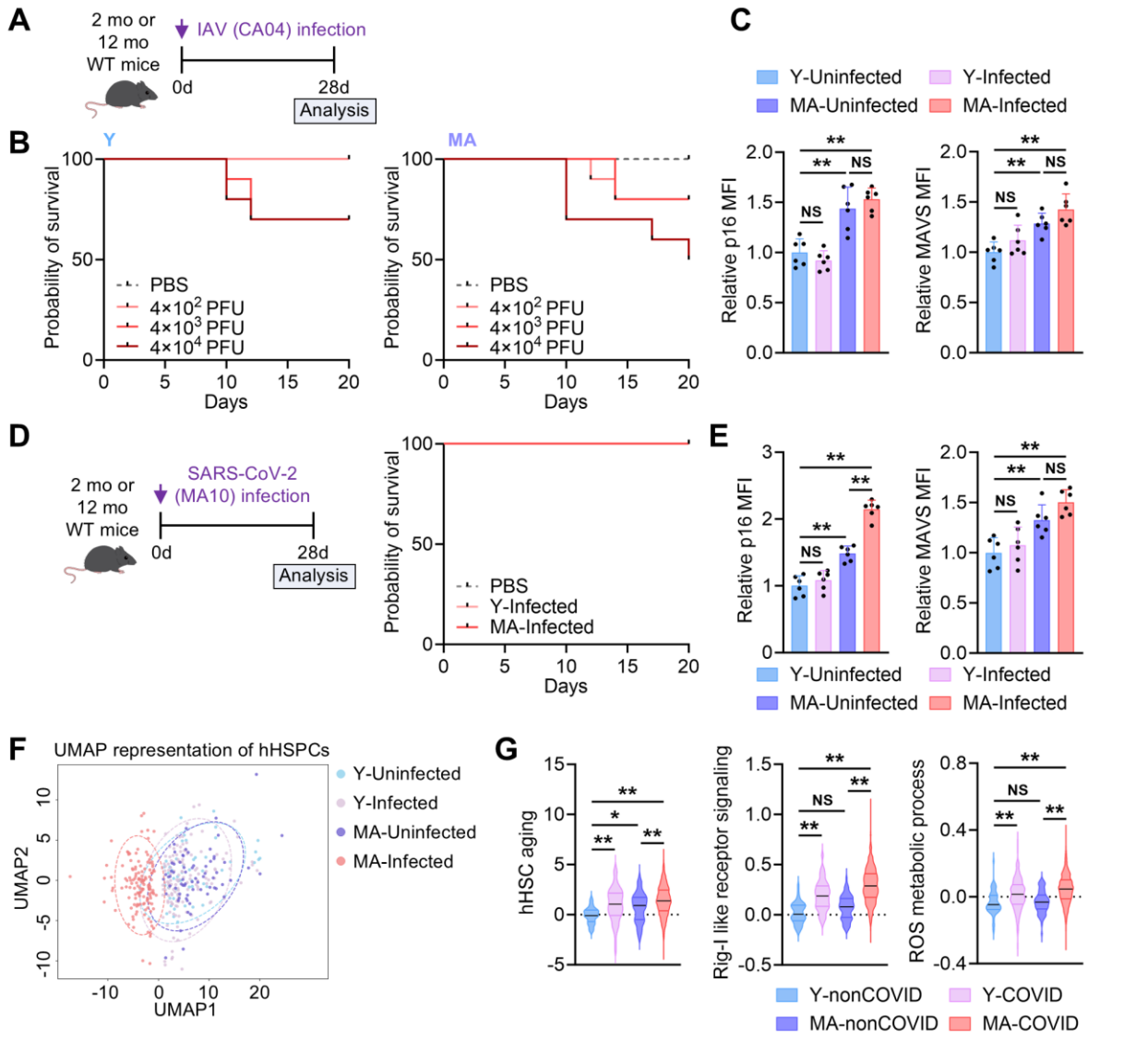
Supplementary Figure 4. *Ex vivo* CCCP treatment attenuates cytosolic mtRNA accumulation and MAVS pathway activation in HSCs. (A) Cytosolic mtRNA levels in HSCs after *ex vivo* CCCP treatment (n = 6). (B) Flow cytometric quantification of phosphorylation level of IRF3 in HSCs after *ex vivo* CCCP treatment (n = 6). (C) Flow cytometric quantification of BIRC6 expression in HSCs from infected MA mice after MitoQ treatment (n = 6). All quantitative data are presented as mean ± SD, one-way ANOVA with Tukey-Kramer post hoc testing was used for multi-group comparisons, *P < 0.05, **P < 0.01. CCCP, carbonyl cyanide m-chlorophenyl hydrazone; mtRNA, mitochondrial RNA.

© 2026. Liao W. et al. Published online at http://www.aginganddisease.org/EN/10.14336/AD.2026.0944



Supplementary Figure 5. Bilobetin partially reversed HSC aging and immunosenescence in IAV-infected middle-aged mice. (A) Flow cytometric quantification of mitochondrial ROS and p16 expression in HSCs from infected MA mice treated with different Bilobetin doses (n = 6). (B) Flow cytometric quantification of BIRC6 expression in infected MA mice following Bilobetin treatment (n = 6). (C) Plasma SASP factor levels (IL-1α, IL-6, MCP-1, CXCL1) in infected MA mice following Bilobetin treatment (n = 6). (D) Experimental schema and flow cytometric analysis of HSC-derived macrophage. BM HSCs isolated at 28 dpi were differentiated into macrophages and stimulated with Poly(I:C), with or without Bilobetin treatment, followed by p16 and IL-6 quantification (n = 6). All quantitative data are presented as mean ± SD, one-way ANOVA with Tukey-Kramer post hoc testing was used for multi-group comparisons, *P < 0.05, **P < 0.01.

© 2026. Liao W. et al. Published online at http://www.aginganddisease.org/EN/10.14336/AD.2026.0944



Supplementary Figure 6. Various HSC phenotypes across different viral strains and types. (A) Experimental schema: young and middle-aged mice were intranasally inoculated with IAV (CA04). (B) Survival curves of Y and MA mice infected with different IAV doses (n = 10). (C) Flow cytometric quantification of p16 and MAVS expression in HSCs at 28 days post infection of IAV (CA04; 4×10^2 PFU) (n = 6). (D) Experimental schema and survival curves of young and middle-aged mice intranasally inoculated with mouse-adapted SARS-CoV-2 strain (MA10; 4×10^3 PFU) (n = 10). (E) Flow cytometric quantification of p16 and MAVS expression in HSCs at 28 days post infection of MA10 (n = 6). (F) UMAP analysis of HSPC transcriptome of young and middle-aged healthy donors (nonCOVID) and COVID patients from scRNA-seq data GSE165080. (G) Aging signature enrichment score analysis of HSC aging, GSEA analysis of RIG-I signaling and ROS signatures of HSPCs from young and middle-aged healthy donors (nonCOVID) and COVID patients (n = 52, 138, 68, and 1614 left to right; n indicates the number of cells). All quantitative data are presented as mean ± SD, one-way ANOVA with Tukey-Kramer post hoc testing was used for multi-group comparisons, *$P < 0.05$, **$P < 0.01$.

© 2026. Liao W. et al. Published online at http://www.aginganddisease.org/EN/10.14336/AD.2026.0944

SUPPLEMENTARY DATA

Supplementary Table 1. Antibodies used for flow cytometry.

Antibody	Origin	Identifier
Biotin Mouse Hematopoietic Lineage Cocktail	eBioscience	Cat# 88-7774-75; RRID: AB_476399
Pacific BlueTM anti-mouse Lineage Cocktail	Biolegend	Cat# 133310; RRID:AB_11150779
PerCP-Cyanine5.5 Anti-Mouse Ly-6A/E (Sca-1)	eBioscience	Cat# 45-5981-82; RRID:AB_914372
PE anti-mouse Ly-6A/E (Sca-1); E13-161.7	Biolegend	Cat#122508; RRID:AB_756193
APC-eFluor 780 Anti-Mouse CD117 (c-Kit)	eBioscience	Cat# 47-1171-82; RRID:AB_1272177
PE-Cyanine7 Anti-Mouse CD117 (c-Kit)	eBioscience	Cat# 25-1171-82; RRID:AB_469644
APC Anti-Mouse CD117 (c-Kit)	eBioscience	Cat# 17-1171-83; RRID:AB_469431
PE Anti-Mouse CD135 (Flt3)	eBioscience	Cat# 12-1351-83; RRID:AB_465860
APC Anti-Mouse CD135 (Flt3)	eBioscience	Cat# 17-1351-82; RRID:AB_10717261
eFluor 660 Anti-Mouse CD34	eBioscience	Cat# 50-0341-82; RRID:AB_10596826
FITC Anti-Mouse CD34	eBioscience	Cat# 11-0341-85; RRID:AB_465022
FITC Anti-Mouse CD48	eBioscience	Cat# 11-0481-85; RRID:AB_465078
Biotin Anti-Mouse CD48	eBioscience	Cat# 13-0481-82; RRID:AB_466470
PE/Cy7 anti-mouse CD150 (SLAM)	BioLegend	Cat# 115914; RRID:AB_439797
Brilliant Violet 421TM anti-mouse CD127 (IL-7Rα)	BioLegend	Cat# 135023; RRID:AB_10897948
APC Anti-Mouse CD41	eBioscience	Cat# 17-0411-80; RRID:AB_1603238
eFluor 450 Anti-Mouse CD45	eBioscience	Cat# 48-0451-82; RRID:AB_1518806
APC-eFluor 780 Anti-human/mouse CD45R (B220)	eBioscience	Cat# 47-0452-82; RRID:AB_1518810
PE-Cyanine7 Anti-Mouse CD3e	eBioscience	Cat# 25-0031-82; RRID:AB_469572
PE Anti-Mouse Ly-6G (Gr-1)	eBioscience	Cat# 12-5931-82; RRID:AB_466045
APC Anti-Mouse CD11b (Mac-1)	eBioscience	Cat# 17-0112-82; RRID:AB_469343
FITC Anti-Mouse CD3e	eBioscience	Cat# 11-0031-82; RRID:AB_464882
APC Anti-Mouse CD3e	Biolegend	Cat#100312; RRID:AB_312677
eFluor 450 Anti-Mouse CD45	eBioscience	Cat# 48-0451-82; RRID:AB_1518806
PE-Cyanine7 Anti-Mouse TER-119	eBioscience	Cat# 25-5921-82; RRID:AB_469661
PerCP-Cyanine5.5 Anti-Mouse CD11c	eBioscience	Cat# 45-0114-82; RRID:AB_925727
PerCP Anti-Mouse CD4	BioLegend	Cat# 100538; RRID:AB_893325
FITC Anti-Mouse CD4	BioLegend	Cat# 100510; RRID:AB_312713
PE Anti-Mouse CD25	BioLegend	Cat# 102008; RRID:AB_312857
APC Anti-Mouse CD25	BioLegend	Cat# 102012; RRID:AB_312861
Pacific BlueTM Anti-Mouse CD8a	BioLegend	Cat# 100725; RRID:AB_493425
Biotin Anti-Mouse NK-1.1	BioLegend	Cat# 108703; RRID:AB_313390
PE anti-mouse FOXP3	BioLegend	Cat# 126404; RRID:AB_1089117
APC anti-Mouse BIRC6	Bioss	Cat# bs-1489R; RRID:AB_10856168
PE anti-mouse IL-6	BioLegend	Cat# 504503; RRID:AB_315337
APC anti-mouse IL-6	BioLegend	Cat# 504508; RRID:AB_315337
Pacific BlueTM anti-mouse p16	Bioss	Cat# bs-23797R; RRID:AB_3743382
Anti-IRF3 Phospho (Ser396)	Proteintech	Cat# 80519-2-RR; RRID:AB_3670478
Anti-TBK1 Phospho (Ser172)	Proteintech	Cat# 82382-2-RR; RRID:AB_3719410
Anti-Mouse MAVS	Proteintech	Cat# 66911-1-Ig; RRID:AB_2882238
PE/Cyanine5 anti-mouse/human CD44	BioLegend	Cat# 103010; RRID:AB_312961
Brilliant Violet 650TM anti-mouse CD62L	BioLegend	Cat# 104453; RRID:AB_2800559
Brilliant Violet 750TM anti-mouse/human B220	BioLegend	Cat# 103261; RRID:AB_2734157
Brilliant Violet 605TM anti-mouse IgD	BioLegend	Cat# 405727; RRID:AB_2562887
Brilliant Violet 421TM anti-mouse IgM	BioLegend	Cat# 406532; RRID:AB_2650930
Brilliant Violet 785TM anti-mouse CD8a	BioLegend	Cat# 100749; RRID:AB_11218801
PerCP/Cyanine5.5 anti-mouse CD4	BioLegend	Cat# 100434; RRID:AB_893324
APC/Cyanine7 anti-mouse CD45	BioLegend	Cat# 103112; RRID:AB_312977
PE/FireTM 640 anti-mouse/human CD11b	BioLegend	Cat# 101280; RRID:AB_2888802
Brilliant Violet 711TM anti-mouse CD279 (PD-1)	BioLegend	Cat# 135231; RRID:AB_2566158
PE anti-mouse CD21/CD35 (CR2/CR1)	BioLegend	Cat# 123409; RRID:AB_940411
APC anti-mouse CD23	BioLegend	Cat# 101620; RRID:AB_2563439
PE/DazzleTM 594 anti-mouse CD43	BioLegend	Cat# 143217; RRID:AB_2800664
PE/Cyanine7 anti-mouse CD93 (AA4.1, early B lineage)	BioLegend	Cat# 136506; RRID:AB_2044012

© 2026. Liao W. et al. Published online at http://www.aginganddisease.org/EN/10.14336/AD.2026.0944

SUPPLEMENTARY DATA

Supplementary Table 2. Primers for mRNA expression analysis.

Gene	Forward primer (5' –3')	Reverse primer (5' –3')
Cdkn2a	GAGCAGCATGGAGCCTTC	CGTAACTATTCGGTGCGTTG
Nd6 (mtRNA)	GGGTTTGGTGGATCGTTTTTAGG	TCCCCAAGTCTCTGGATATTCCT
12S (mtDNA)	ACCGCGGTCATACGATTAAC	CCCAGTTTGGGTCTTAGCTG
Hprt	TCAGTCAACGGGGGACATAAA	GGGGCTGTACTGCTTAACCAG

© 2026. Liao W. et al. Published online at http://www.aginganddisease.org/EN/10.14336/AD.2026.0944